THE ASTROPHYSICAL JOURNAL, 408:548–558, 1993 May 10

CHEMICAL DIFFERENTIATION BETWEEN STAR-FORMING REGIONS: THE ORION HOT CORE AND COMPACT RIDGE

P. CASELLI,[1,2] T. I. HASEGAWA,[1] AND ERIC HERBST[1,3]

Received 1992 August 28; accepted 1992 November 2

ABSTRACT

We present a dynamical-chemical model of massive star-forming regions, in which gas and dust grains are included. We consider the last 10^5 yr of the accretion phase of a protostellar object embedded in a dense and massive cloud with a density and temperature gradient. We follow the gas and grain chemical evolution of two collapsing shells of this cloud, until the end of the protostar accretion phase, at which time the density no longer increases. At this point, the temperature rises, the molecular mantles of the grains evaporate, and we follow the time evolution of the resultant gas chemistry. The scenario is based on earlier models of Millar, Brown, Charnley, and Tielens. We find that differences in thermal history during the gravitational collapse of the two circumstellar shells can lead to chemical differentiation between the Orion Hot Core and Compact Ridge, two clumps of OMC-1 very close to the luminous infrared source IRc2. Detailed comparison between our model results and observations of these two sources shows a mixed pattern of agreement and disagreement. The adoption of dynamical histories to achieve good agreement with observation for the abundances of the complex organic molecules leads to some large discrepancies for small species such as NH_3.

Subject headings: ISM: abundances — ISM: molecules — molecular processes — stars: formation — stars: pre–main-sequence

1. INTRODUCTION

Recent gas-grain models of interstellar chemistry in dense and quiescent clouds (Hasegawa, Herbst, & Leung 1992; Herbst 1993; Hasegawa & Herbst 1993) reproduce observations of CO and H_2O ices in the Taurus region reasonably well. They are also successful in reproducing observed gas phase abundances in TMC-1 (see Herbst & Leung 1990). In these pseudo-time dependent models the dust and gas temperature is fixed at 10 K and the gas density $n = n(H) + 2n(H_2)$ remains approximately at 2×10^4 cm^{-3}. Desorption via impulsive cosmic ray heating of the entire grains (Léger, Jura, & Omont 1985), together with thermal desorption, have been considered. At the low temperatures typical of quiescent interstellar clouds, the gas phase is almost totally depleted of complex neutral molecules after a sufficient period of time ($\sim 10^7$ yr).

Here we focus on star-forming regions, in which higher temperatures and densities can seriously alter the chemistry compared with that of quiescent clouds. Small ($\sim$0.1 pc), dense ($\sim 10^7$ cm^{-3}), and hot ($T \sim$ 100–200 K) clumps have been recently detected in star-forming molecular clouds (Sweitzer 1978; Pauls et al. 1983; Henkel et al. 1987; Jacq et al. 1990). In general, the strongest spectral signatures of these regions are the enhanced abundances of certain polyatomic molecules relative to their abundances in cold, dark clouds (Walmsley 1989). For example, Pauls et al. (1983) detected emission from metastable transitions of NH_3 in the Orion-KL region. They concluded that NH_3 emission came from a hot, dense region, and they suggested that the fractional abundance of ammonia, about two orders of magnitude larger than that observed in cold, dark clouds, arose from the evaporation of molecular mantles on interstellar grains. The same interpretation, based on the release of surface species into the gas phase, was used to explain the enhanced abundances of methanol, CH_3OH (Menten et al. 1986) and deuterated water, HDO (Olofsson 1984; Moore, Langer, & Huguenin 1986; Henkel et al. 1987) in hot clumps close to young stellar objects, generally called "hot cores." Although there are several similarities involving density, temperature, and size among these "hot cores," there are also some striking differences in chemical abundances (Blake et al. 1987; Irvine, Goldsmith, & Hjalmarson 1987; Genzel & Stutzki 1989), suggesting that some physical parameter must play an important role in determining the different chemical evolution of different star-forming clouds or, more surprisingly, of different parts of the same star-forming cloud. In this paper, we try to reproduce the well-known chemical differentiation between two clumps of the Orion-KL cloud core, very close to the luminous ($L \sim 10^5\ L_\odot$), and massive ($M \sim 25\ M_\odot$) young stellar object IRc2: the Hot Core and the Compact Ridge.

The Hot Core is a particularly warm ($T \sim 200$ K), compact (angular size less than 10″), and dense ($n \geq 10^7$ cm^{-3}) region of material centered $\sim$2″ southeast of IRc2 (Wright et al. 1992). This clump may be the remnant of the dense parental cloud out of which IRc2 has formed and that now interacts with its outflow and radiation (Genzel & Stutzki 1989). The chemistry of the Hot Core is characterized by unusually high abundances of H-rich complex nitrogen-bearing molecules, such as vinyl cyanide (CH_2CHCN) and ethyl cyanide (CH_3CH_2CN) (Blake et al. 1987).

The Compact Ridge is a 15″ size condensation of gas ($n \geq 10^6$ cm^{-3}) extending to the southeast of the Hot Core (Wright et al. 1992). It is warmer ($T \sim 100$ K) than the rest of the Orion Ridge ($T \sim 50$ K), and it is characterized by high abundances of large oxygen-bearing molecules; namely, methanol (CH_3OH), methyl formate ($HCOOCH_3$), and dimethyl

[1] Department of Physics, The Ohio State University, 174 West 18th Avenue, Columbus, OH 43210-1106.
[2] Dipartimento di Astronomia, Università di Bologna, Via Zamboni 33, 40126 Bologna, Italy.
[3] Department of Astronomy, The Ohio State University, 174 West 18th Avenue, Columbus, OH 43210-1106.

ether (CH_3OCH_3) (Blake et al. 1987). The Compact Ridge also contains several CH_3OH masers (Plambeck & Wright 1987; Menten et al. 1988). Blake et al. (1987) suggested that this clump was created by an interaction of the outflowing material from IRc2, the so-called Plateau source, with the quiescent gas of the Orion Ridge. Such an interaction is also made plausible by the spatial coincidence between the Compact Ridge and the low-velocity H_2O masers, that could be the locations of clump-cloud shocks (Genzel & Stutzki 1989).

Several attempts have been made to model these regions chemically (e.g., Brown, Charnley, & Millar 1988; Brown 1990; Millar, Herbst, & Charnley 1991; Charnley, Tielens, & Millar 1992). The basic idea of most of these previous models is to follow the chemical evolution of a cold ($T = 10$ K) collapsing clump of gas and dust until some heating event, associated with the formation of a nearby star, liberates the molecular mantles into the gas phase (Brown et al. 1988). However, different initial abundances of key molecules (NH_3, CH_3OH; Charnley et al. 1992) after mantle evaporation, or injection of methanol (Millar et al. 1991), were needed to reproduce the different chemical compositions of the Hot Core and the Compact Ridge.

In this paper, we discuss a more unified view of the varying chemical compositions. In particular, we consider a massive spherical cloud containing a luminous protostar able to heat the circumstellar environment. Following the radiative transfer calculations of Scoville & Kwan (1976), we assume that the cloud has a density and temperature gradient, and we fix our attention on two distinct shells of this cloud. If the central protostar is in its accretion phase, these two shells will collapse in free-fall and increase their density until the inversion of the inflow, likely due to radiation or powerful stellar winds able to halt the accretion (Larson & Starrfield 1971; Lada 1985; Shu, Adams, & Lizano 1987; Churchwell 1991). The interaction of the shells with the outflowing material, together with their decreased distance from the stellar heating source, causes a sudden increase of temperature and the release of surface molecules into the gas phase.

In the next sections we show how the assumed different thermal conditions during the gravitational collapse can lead to different spectral signatures in the Orion Hot Core and Compact Ridge.

2. MODEL

2.1. *Chemical Network*

The model results have been obtained by solving coupled kinetic differential equations of the type (Hasegawa et al. 1992):

$$dn(i)/dt = \Sigma_l \Sigma_j K_{lj}\, n(l) n(j) - n(i) \Sigma_j K_{ij}\, n(j) - k_{acc}(i) n(i) + \{k_{evap}(i) + k_{crd}(i)\} n_s(i) \quad (1)$$

$$dn_s(i)/dt = \Sigma_l \Sigma_j k_{lj}\, n_s(l) n_s(j) - n_s(i) \Sigma_j k_{ij}\, n_s(j) + k_{acc}(i) n(i) - \{k_{evap}(i) + k_{crd}(i)\} n_s(i)\,, \quad (2)$$

where $n(i)$ and $n_s(i)$ are, respectively, the gas and the surface concentration of species i; K_{lj} and k_{lj} are, respectively, the gas phase and surface rate coefficients of reactions between species l and j; $k_{acc}(i)$ is the grain accretion rate for species i, $k_{evap}(i)$ is the thermal evaporation rate for species i, and $k_{crd}(i)$ is the cosmic-ray induced nonthermal desorption rate coefficient for species i. All rate coefficients have been discussed extensively in Hasegawa et al. (1992). Unlike the 10 K grains studied by Hasegawa et al. (1992), and by Hasegawa & Herbst (1993), the warmer grains ($20 \leq T \leq 40$ K) here permit thermal evaporation of selected surface species to occur rapidly during the collapse phase and to affect the chemistry severely The desorption energies utilized in this work are listed in Table 3 of Hasegawa & Herbst (1993) except for the newly added value for methyl formate, which has been estimated to be 3100 K.

The elemental abundances used to describe the gas phase and the grain mantle are the so-called "low-metal" abundances (Graedel, Langer, & Frerking 1982; Leung, Herbst, & Huebner 1984). We assume a sticking probability of 1.0 for all neutral atoms and molecules that strike a grain during the low temperature (collapse) phase.

Schematically, the chemical scenario on grains is the following: gas phase neutral atoms and molecules (1) accrete onto surfaces of classical grains, (2) migrate from potential wells to adjacent wells on grain surfaces, (3) encounter reaction partners, (4) react to form molecules that are nomally more complex. Thermal evaporation and nonthermal desorption via impulsive cosmic ray heating of the entire grain (Leger, Jura, & Omont 1985; Hasegawa & Herbst 1993) return surface molecules to the gas phase. The effect of the cosmic ray desorption is negligible compared with thermal desorption or values of the temperature greater than 20 K.

There are 255 surface reactions in our chemical network, involving 146 neutral surface species. These are discussed in Hasegawa & Herbst (1993) and Hasegawa et al. 1992). Some examples are addition reactions with atomic carbon and nitrogen,

$$C + C_n \rightarrow C_{n+1} (n \geq 1) \quad (3)$$

$$N + C_n \rightarrow C_n N (n \geq 1)\,, \quad (4)$$

and the hydrogenation of unsaturated radicals to form more stable saturated forms:

$$C_n + H \rightarrow HC_n \quad (5)$$

$$C_n N + H \rightarrow HC_n N \quad (6)$$

$$HC_n + H \rightarrow C_n H_2\,. \quad (7)$$

For hydrocarbons with more than one carbon atom, we also consider the following surface reactions:

$$C_n + H_2 \rightarrow C_n H + H \quad (8)$$

$$C_n H + H_2 \rightarrow C_n H_2 + H \quad (9)$$

where $2 \leq n \leq 9$, with activation energies of 2100 K (Hasegawa & Herbst 1993). Surface formation of the saturated species C_2H_5CN via hydrogenation of HC_3N is considered due to the observed high abundance of the former species in the Hot Core. Although analogous saturated organo-nitrogen species with more carbon atoms are also produced on grains, they are not included in the model, which artificialy limits the degree of saturation to the species $H_3C_{2n+1}N$ for $n > 1$.

The surface reaction network is combined with our gas phase reaction network that consists of 2918 reacions involving 304 gas phase species. In particular, for the complex O-bearing molecules, the gas phase network contains the reactions

$$CH_3OH_2^+ + H_2CO \rightarrow H_2COOCH_3^+ + I_2 \quad (10)$$

$$CH_3OH_2^+ + CH_3OH \rightarrow (CH_3)_2OH^+ + H_2O\,. \quad (11)$$

that lead to methyl formate and dimethyl ether, respectively, upon dissociative recombination (Millar et al. 1991).

2.2. *Dynamical Evolution*

We assume that the central protostar is accreting matter from the surrounding envelope, which continues to collapse at the free-fall rate. Because of the existence of a density gradient in the cloud, the free-fall time is different for different mass shells; the inner regions will collapse first, whereas the outer ones will fall in at progressively later times (Spitzer 1978). In this situation we have to distinguish between the initial density of the shell, or the initial "chemical density," and the initial mean density within a sphere of radius equal to the radius of the shell, or initial "dynamical density." This "dynamical density," $n_{\rm dyn}$, regulates the free-fall rate by entering into the formulas that describe the collapse. In the calculations discussed below, the solution to the free-fall equation is approximated by the empirical equation

$$n_{\rm dyn}(t)/n_{\rm dyn}(0) = \{1 - [t/t_{\rm ff}]^{2.1}\}^{-2}\,, \qquad (12)$$

where $t_{\rm ff}$ is the standard free-fall time (Spitzer 1978). On the other hand, the initial "chemical density" is one of the parameters that determines the initial conditions at the starting point of our chemical calculations. The ratio of chemical density to dynamical density is fixed during the collapse phase. With this method we can approximately simulate a nonhomologous collapse of the cloud, after the formation of the central "embryo star" that continues to grow in mass through accretion of the remaining protostellar material (Larson 1969, 1972).

We follow the chemistry of two separated cloud shells during their dynamical evolution lasting 10^5 yr. After 10^5 yr we assume that the protostar accretion phase is finished, and that the two shells stop collapsing and heat up due to interaction with IRc2. The two shells represent the Orion Hot Core and Compact Ridge (Fig. 1).

For the Hot Core we start with a dense ($n = 1 \times 10^5$ cm^{-3}), warm ($T_{\rm gas} = T_{\rm dust} = 40$ K) shell, in which all the hydrogen is in molecular form and the easily ionized heavy atoms are found in their ionized form. Considering an accretion rate $dM/dt \sim 10^{-5}\ M_\odot$ yr^{-1} (Stahler, Shu, & Taam 1980; Shu, Adams, & Lizano 1987) and current mass $M = 25\ M_\odot$ for IRc2, and the mass-luminosity relation $L_*/L_\odot = (M_*/M_\odot)^{3.3}$ (Allen 1963), we can estimate the initial mass (M_i) and luminosity (L_i) of IRc2 at the starting point of our calculation, i.e., 10^5 yr before the end of the accretion phase. We obtain $M_i = 24\ M_\odot$, and $L_i = 8.7 \times 10^4\ L_\odot$. With these values of M_i and L_i, and with the temperature and density relations of Scoville & Kwan (1976), the Hot Core shell can be located at an average distance $r_i = 0.24$ pc from the central protostar with a dynamical density of about 2×10^5 cm^{-3}, at the beginning of the calculation. At the end of the accretion phase, the Hot Core shell has increased its chemical density to 1.3×10^7 cm^{-3}, and decreased its distance from IRc2 to $\sim 5 \times 10^{-2}$ pc. At this point, it interacts with the outflowing material and/or radiation from IRc2; the resultant effect is assumed to be a sudden increase of dust and gas temperature ($T = 200$ K) and the evaporation of the grain mantles. Then we follow the gas phase chemistry at our assumed temperature of 200 K and constant (chemical) density $n = 1.3 \times 10^7$ cm^{-3} for 10^6 yr.

For the Compact Ridge, the initial chemical density ($n = 2.0 \times 10^4$ cm^{-3}) and temperature ($T_{\rm gas} = T_{\rm dust} = 20$ K)

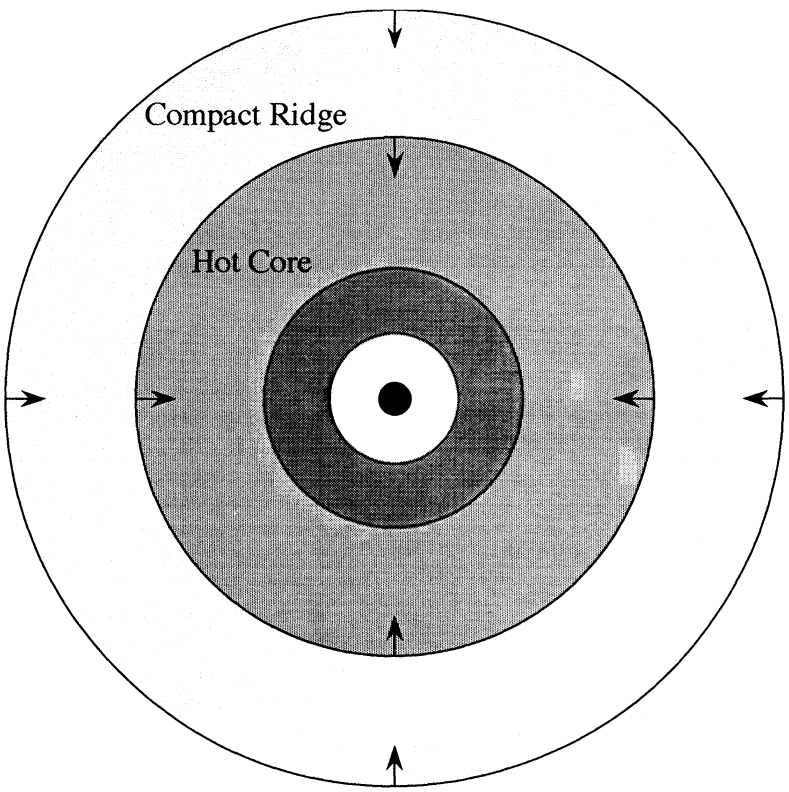

FIG. 1.—Schematic picture of the cloud at the beginning of the calculation. The cloud is a spherical shell, with a density and temperature gradient (*shaded region*), centered on the star. From the star to the cloud a wind-blown central cavity exists (*white region*). The Orion Hot Core and Compact Ridge are depicted as two different shells of the same collapsing cloud.

were chosen considering this region as a more external shell of the same collapsing cloud (Fig. 1). Here the hydrogen is initially in atomic form. With the same approach used for the Hot Core, we locate the initial Compact Ridge shell at an average distance $r_i = 1.38$ pc from IRc2 and a dynamical density of 3×10^4 cm^{-3}. With this value of the dynamical density, a free-fall lasting about 3×10^5 yr is needed to increase the Compact Ridge chemical density to 10^6 cm^{-3}; however, to avoid complicating our oversimplified dynamical model, we consider a faster dynamical contraction so that the Compact Ridge shell and the Hot Core shell will cease their collapse at the same time of 10^5 yr. This further approximation does not play an important role in the final chemical results. With this simplification, the chemical density of the Compact Ridge reaches 10^6 cm^{-3} after 1×10^5 yr. At this time, $r \sim 0.37$ pc and temperature is assumed to be raised suddenly to $T = 100$ K. This temperature is high enough so that the surface molecules are evaporated, and the gas phase chemistry is followed for 10^6 yr at $T = 100$ K and (chemical) density fixed at $n = 1.0 \times 10^6$ cm^{-3}.

3. RESULTS

In Table 1 the theoretical results at 3.2×10^4 yr and 1.0×10^5 yr after evaporation are compared with observed

TABLE 1

COMPARISON WITH OBSERVATIONS OF THE ORION HOT CORE AND COMPACT RIDGE

Species	FRACTIONAL ABUNDANCES							
	COMPACT RIDGE				HOT CORE			
	Observed	Ref.	Theory		Observed	Ref.	Theory	
			3.2 10^4 yr	1.0 10^5 yr			3.2 10^4 yr	1.0 10^5 yr
CN	3.3(-9)[a]	1	**3.6(-10)**	1.5(-9)	<5.0(-10)	1	6.6(-12)	**3.1(-12)**
CO	5.0(-5)[a]	1	**2.8(-5)**	3.0(-5)	1.2(-4)	1	1.4(-4)	**1.4(-4)**
O_2	--		**7.7(-6)**	1.7(-5)	<1.0(-4)	1	1.4(-5)	**2.6(-5)**
CS	2.5(-9)[a]	1	**8.8(-10)**	3.1(-9)	<5.5(-10)	1	6.2(-13)	**3.7(-13)**
SO	≤9.3(-10)[a]	1	**3.8(-8)**	7.7(-9)	≤2.0(-8)	1	1.7(-8)	**2.6(-8)**
H_2O	1.0(-4)	2	**2.5(-4)**	2.5(-4)	≥5.3(-6)	1	4.9(-6)	**1.2(-6)**
C_2H	5.3(-9)[a]	1	**3.9(-11)**	3.3(-9)	<5.5(-10)	1	2.5(-13)	**1.7(-13)**
HCN	5.0(-9)[a]	1	**6.1(-7)**	5.0(-7)	3.0(-7)	1	4.2(-10)	**1.7(-10)**
HNC	5.3(-10)[a]	1	**3.2(-7)**	3.4(-7)	1.0(-9)	3	3.6(-9)	**3.8(-10)**
CO_2	--		**9.7(-7)**	1.5(-6)	<1.0(-5)	1	7.0(-7)	**7.1(-7)**
OCS	3.3(-9)	1	**9.2(-9)**	9.1(-9)	--		1.5(-9)	**3.4(-10)**
SO_2	≤3.3(-9)[a]	1	**1.2(-8)**	4.7(-8)	≤2.4(-8)	1	1.3(-7)	**1.3(-7)**
NH_3	6.7(-8)	4	**2.3(-5)**	1.2(-5)	5.7(-7)	5	1.3(-9)	**3.3(-9)**
H_2CO	3.7(-8)	6	**2.0(-5)**	1.9(-5)	2.6(-8)	1	1.2(-8)	**4.5(-9)**
HNCO	--		**8.3(-8)**	8.1(-8)	5.8(-9)	1	1.6(-8)	**1.1(-8)**\
H_2CS	1.6(-9)	1	**9.2(-8)**	8.9(-8)	--		1.9(-9)	**4.3(-10)**
C_3N	<1.7(-11)[a]	1	**1.5(-12)**	5.2(-10)	--		3.0(-12)	**1.3(-12)**
CH_4	--		**7.5(-5)**	7.5(-5)	<1.0(-5)	1	5.7(-7)	**4.8(-7)**
CH_2CO	6.7(-10)	1	**9.7(-9)**	1.8(-8)	--		2.2(-8)	**4.5(-9)**
HCOOH	5.0(-10)	1	**1.3(-10)**	3.9(-10)	--		5.6(-9)	**1.4(-9)**
C_4H	<1.3(-10)	7	**4.5(-13)**	7.7(-11)	--		1.2(-14)	**9.8(-15)**
HC_3N	1.3(-10)[a]	1	**1.8(-9)**	2.1(-8)	1.6(-9)	1	1.5(-8)	**1.8(-9)**
CH_3OH	1-10(-7)	8	**2.0(-5)**	1.8(-5)	--		1.0(-10)	**9.2(-12)**
CH_3CN	3.2(-10)	1	**5.9(-9)**	1.6(-8)	7.8(-9)	1	3.6(-8)	**1.4(-10)**
CH_3NH_2	<1.0(-9)	1	**1.5(-7)**	2.1(-7)	--		4.1(-11)	**6.5(-12)**
C_3H_4	2.0(-9)[a]	7	**1.2(-9)**	1.3(-9)	--		1.1(-8)	**1.4(-9)**
CH_3CHO	<1.7(-10)	1	**2.0(-8)**	1.9(-8)	--		1.1(-11)	**1.2(-12)**
CH_2CHCN	--		**1.8(-10)**	4.8(-9)	1.8(-9)	1	1.4(-8)	**1.8(-9)**
HC_5N	2.3(-11)[a]	7	**2.5(-11)**	3.2(-10)	--		7.7(-10)	**3.0(-11)**
CH_3OCH_3	1.0(-8)	1	**1.3(-8)**	3.8(-8)	--		1.0(-13)	**1.8(-14)**
C_2H_5OH	<5.0(-10)	1	**8.5(-12)**	2.7(-11)	--		4.4(-13)	**2.9(-13**
CH_3CH_2CN	--		**1.0(-9)**	8.4(-10)	9.8(-9)	1	9.8(-8)	**2.4(-8)**
$HCOOCH_3$	8.7(-9)	1	**3.7(-8)**	8.4(-8)	--		1.3(-13)	**1.9(-14)**
HCO^+	--		**9.7(-13)**	9.7(-13)	<5.0(-10)	1	6.5(-11)	**2.8(-10)**
H_3O^+	5.0(-9)	9	**2.3(-10)**	3.5(-10)	--		8.7(-10)	**8.0(-10)**
e	--		**5.1(-9)**	5.0(-9)	--		1.4(-9)	**1.5(-9)**

NOTES:—$a(-b)$ refers to $a \times 10^{-b}$. Fractional abundances are relative to $H_2 + 0.5$ H.

[a] For the Orion Extended Ridge; reliable observations are unavailable for the Compact Ridge.

REFERENCES:—(1) Blake et al. 1987; Moore et al. 1986; (3) Goldsmith et al. 1986; (4) Turner 1990; (5) Walmsley et al. 1987; (6) Magnum et al. 1990; (7) Johansson et al. 1984; (8) Menten et al. 1988; (9) Wootten et al. 1991.

molecular fractional abundances in the Hot Core and Compact Ridge; the more favorable times are listed in bold for each source -3.2×10^4 yr for the Compact Ridge, and 1.0×10^5 yr for the Hot Core. For several molecules not observed directly in the Compact Ridge, we adopted fractional abundances found in the Orion Extended Ridge. In effect, the distinction between the Extended and Compact Ridge is often ill-defined, especially for the simpler species which possess extended emission (Blake et al. 1987).

From the table we note mixed agreement with observations. The agreement is best for complex molecules. In the Hot Core, 10^5 yr after the evaporation of the grain mantles, calculated abundances of vinyl cyanide (CH_2CHCN) and ethyl cyanide (CH_3CH_2CN), two complex N-bearing molecules, are very close to the large observed values, whereas the complex O-bearing molecules are under the detectability limit. For the Compact Ridge we obtain good agreement with the observed large abundances of $HCOOCH_3$ and CH_3OCH_3, 3.2×10^4 yr after the evaporation; here the complex N-bearing molecules are one order of magnitude less abundant than in the Hot Core. If the calculated abundances of the Compact Ridge at 10^5 yr after grain mantle evaporation are utilized, the complex O-bearing molecules and several complex N-bearing species, such as HC_5N, have abundances that are somewhat large compared with observation; indeed, the abundance of vinyl cyanide (CH_2CHCN) increases to a level equivalent to its value in the Hot Core. In the Hot Core, contrary to the situation of the Compact Ridge, important molecular abundances decrease going from 3.2×10^4 to 1.0×10^5 yr; for some lighter species such as HNC and H_2CO the best agreement with observations is at 3.2×10^4 yr; however, from Table 1 we see that the theoretical fractional abundances are generally overestimated at this earlier time, in particular the vinyl cyanide and ethyl cyanide abundances are one order of magnitude larger than at 1.0×10^5 yr.

The differing times for best agreement with observations in the Hot Core and the Compact Ridge may reflect a real difference in the time of grain mantle release between the two regions. In effect, the Hot Core, being closer to Irc2, could have interacted with the outflowing material from the central star before the Compact Ridge. In particular, the adopted difference between optimum post mantle evaporation times for the Hot Core and the Compact Ridge is 6.8×10^4 yr; this value is only 4 times larger than the time delay obtained by dividing the approximate distance between the two regions, achieved at the end of our dynamical calculation ($\Delta r \sim 0.32$ pc), by the velocity of the outflow interacting with the two studied clumps ($v \sim 18$ km s^{-1}; Genzel & Stutzki 1989).

The calculated abundances in Table 1 result from gas phase and grain chemistry occurring in the isothermal gravitational collapse phase as well as gas chemistry in the constant-density high-temperature phase. In Figures 2 and 3 the time evolution of the most abundant O-bearing and N-bearing molecules in the two cloud shells during the gravitational collapse phase are shown. Figures 2*a* and 3*a* show the different behavior of surface species in the Hot Core and the Compact Ridge, respectively. The equivalent figures for the gas phase species are shown as Figures 2*b* and 3*b*. During the gravitational collapse, the surface chemistry in the two shells is very different from each other, leading to high surface abundances of vinyl and ethyl cyanide, and cyanoacetylene in the Hot Core (Fig. 2*a*), whereas the grain mantles in the Compact Ridge shell become rich with water, ammonia, methanol, and formaldehyde (Fig. 3*a*). The fractional abundance of the most abundant surface species in the Compact Ridge at the end of the collapse (H_2O), however, is more than three orders of magnitude greater than that of the most abundant surface species in the Hot Core at the end of the collapse (CH_3CH_2CN). This reflects the higher initial temperature considered in the Hot Core, which is exponentially linked to the evaporation rate of the surface molecules (see eq. [2] in Hasegawa, Herbst, & Leung 1992); therefore, the molecular fractional abundances on the grain surfaces will tend to be smaller in the warmer region. The gas composition of the two collapsing shells is also completely different: the Compact Ridge is dominated by ammonia (Fig. 3*b*), whereas the most abundant gas phase molecules in the Hot

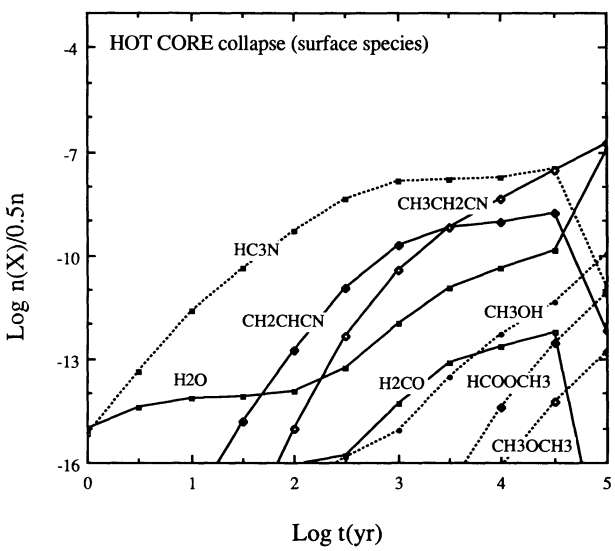

FIG. 2*a*

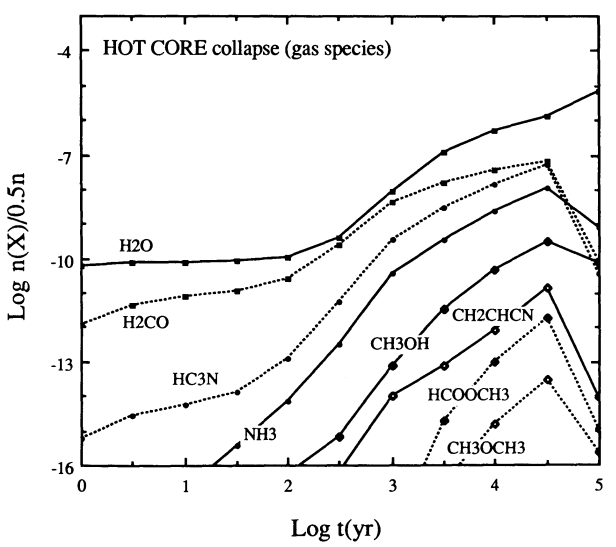

FIG. 2*b*

FIG. 2.—Time evolution of the fractional abundances of important N-bearing and O-bearing (*a*) surface and (*b*) gas phase species for the Orion Hot Core during the gravitational collapse.

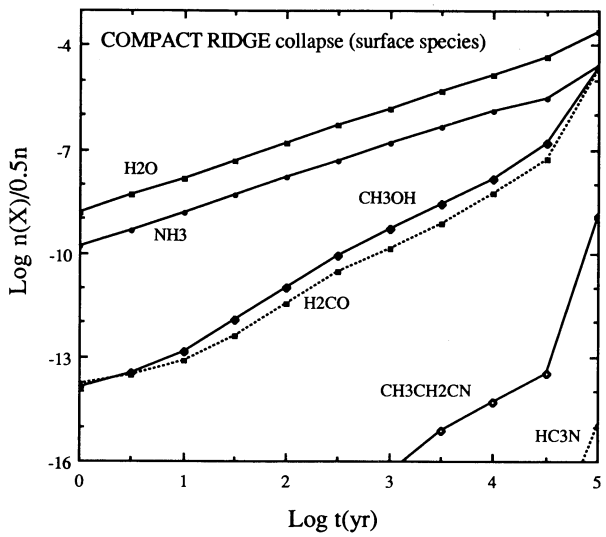

FIG. 3a

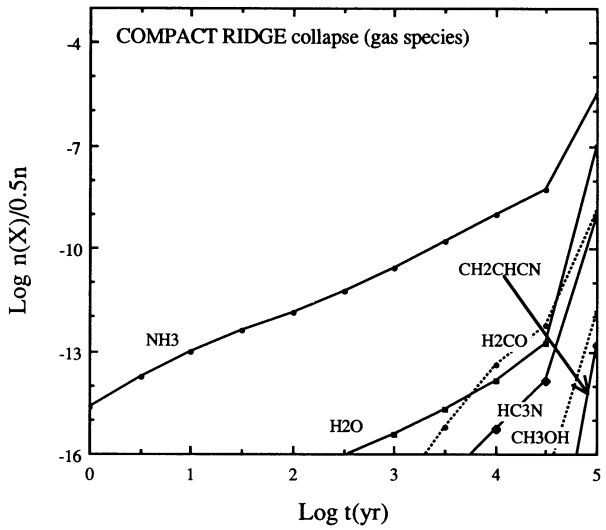

FIG. 3b

FIG. 3.—Time evolution of the fractional abundances of important N-bearing and O-bearing (*a*) surface and (*b*) gas phase species for the Orion Compact Ridge during the gravitational collapse.

Core are water, formaldehyde, and cyanoacetylene (Fig. 2*b*). As in the case of the surface molecules, Figures 2*b* and 3*b* reflect the difference in temperature of the two regions. In the Hot Core, gas phase chemistry plays a more important role than in the Compact Ridge, given the higher evaporation rates of the molecules, especially the lighter ones. In the Hot Core, species like ammonia, water, formaldehyde, and cyanoacetylene are primarily formed in the gas, whereas the formation of the same molecules in the Compact Ridge is mostly linked to surface chemical processes followed by evaporation. From Figures 2*a* and 2*b* we note that the higher initial density in the Hot Core compared with the Compact Ridge allows the gaseous molecules, and some surface molecules like H_2CO and HC_3N coupled to the gaseous ones through accretion and efficient evaporation at $T = 40$ K, to reach well-known "early time" peaks at about 3×10^4 yr after the start of the collapse, at which time complex molecules reach their maximum abundances (Leung, Herbst, & Huebner 1984; Herbst & Leung 1989). On the other hand, the Compact Ridge shell density during the gravitational collapse does not permit the gas phase species to reach their peak abundances before the inversion of the inflow (see Fig. 3*b*). Although not emphasized here, it is entirely possible that the collapse phase of our calculations corresponds to other sources in which the central protostar has not yet stabilized the contraction. In particular, the high gaseous ammonia abundance predicted for late stages of the Compact Ridge collapse might be a signature of such phases, although it rests on our small adopted adsorption energy for surface ammonia (Hasegawa & Herbst 1993).

In Figures 4 and 5, the time dependence of selected gas phase abundances after grain mantle evaporation in the Hot Core and Compact Ridge, respectively, is shown. In both regions, many molecular abundances remain relatively constant for at least 10^4 yr. In the Compact Ridge, however, the complex O-bearing molecules $HCOOCH_3$ and CH_3OCH_3 increase their abundances sharply on a short time scale via ion-molecule processes starting from CH_3OH and H_2CO, which maintain very high abundances (Millar et al. 1991). In the Hot Core (and to a lesser extent the Compact Ridge), vinyl cyanide (CH_2CHCN) is formed rapidly from copious amounts of ethyl cyanide (CH_3CH_2CN) via reactions such as

$$H^+ + CH_3CH_2CN \rightarrow C_3H_4N^+ + H_2 \quad (13)$$

$$H_3^+ + CH_3CH_2CN \rightarrow C_3H_4N^+ + 2H_2 \quad (14)$$

followed by dissociative recombination of the $C_3H_4N^+$ into C_3H_3N (CH_2CHCN) and H.

After 10^5 yr, many of the molecules in the Hot Core tend to decrease sharply in abundance. This decrease is related to the transitory nature of large abundances of organic molecules in ion-molecule chemistry as well as the higher density of the Hot Core compared with the Compact Ridge. In general, the fractional ionic abundance is inversely proportional to the square root of the overall gas density, so that the absolute ion density

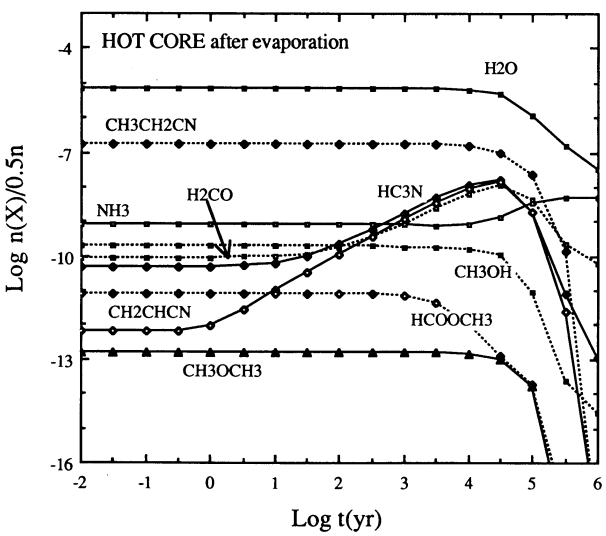

FIG. 4.—Time evolution of the fractional abundances of important N-bearing and O-bearing gas phase species for the Hot Core after the evaporation of the grain mantles.

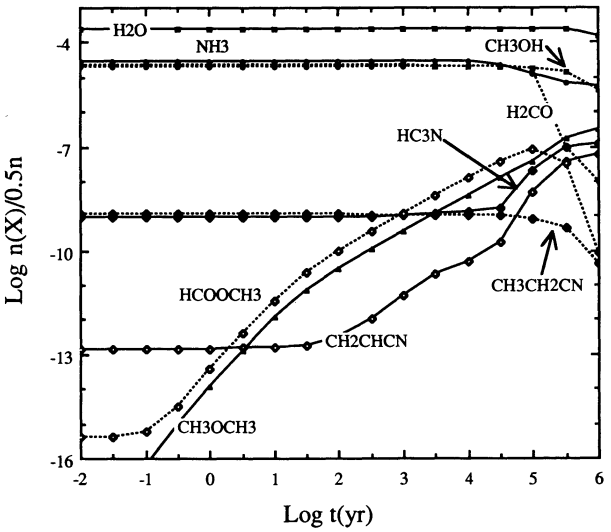

FIG. 5.—Time evolution of the fractional abundances of important N-bearing and O-bearing gas phase species for the Compact Ridge after the evaporation of the grain mantles.

increases as the square root of the density (Leung, Herbst, & Huebner 1984). Thus, the ion-molecule chemistry proceeds in general more rapidly in the Hot Core.

4. DISCUSSION

The chemical differentiation between the Orion Hot Core and Compact Ridge can be better understood by looking at the schematic diagrams of surface chemical pathways in Figures 6 and 7. Figure 6*a* shows the most important pathways that lead to the formation of O-bearing molecules such as CH_3OH and H_2CO in the Compact Ridge during the collapse phase; an analogous diagram for the Hot Core is shown in Figure 6*b*. In these figures the gas phase is represented by shaded circles. The molecules CH_3OH and H_2CO are precursors for the formation of methyl formate and dimethyl ether through gas phase reactions (10) and (11). From Figure 6*b* we can infer that the higher temperature of the Hot Core during gravitational collapse leads to an increase in the evaporation rates of the lighter and more volatile O-containing species. In particular, for CO, this drastically reduces the rate of the surface processes

$$CO \rightarrow HOC \rightarrow HOCH \rightarrow HOCH_2 \rightarrow CH_3OH \quad (15)$$

$$CO \rightarrow HCO \rightarrow H_2CO\ . \quad (16)$$

The surface syntheses are so inefficient that H_2CO and CH_3OH are formed mainly in the gas and then accreted onto the grain surfaces where they remain unreactive. Therefore, in the Hot Core, the O-bearing molecules are almost unaffected by grain chemistry.

This is not true at 20 K, the initial temperature of the Compact Ridge (Fig. 6*a*). At this value of the temperature, CO remains on grain surfaces long enough so that formation of large amounts of methanol and formaldehyde is mainly due to the rapid surface hydrogenation of CO, through the surface processes (15) and (16), leading, consequently, to high abundances for the related species $HCOOCH_3$ and CH_3OCH_3 after the evaporation of the grain mantles.

In general, the surface chemistry at $T = 40$ K in the Hot Core resembles Model D of Hasegawa et al. (1992). In Model D, hydrogenation of the heavy atoms C, N, O is slow enough that these reactive atoms can combine with one another to form reactive diatomic species, which can further combine to form unsaturated polyatomic molecules. Hydrogenation eventually occurs, but it is not rapid enough to interfere with the synthesis of complex species. The slowness of hydrogenation in the Hot Core is due to the low surface abundances of the volatile species H and H_2. In the Compact Ridge, on the other hand, H and H_2 have higher surface abundances and the surface pathways to molecular complexity are less pronounced. This aspect can be seen in Figure 7, where the most important processes related to the production of multicarbon N-bearing complex molecules in the Compact Ridge (Fig. 7*a*), and in the Hot Core (Fig. 7*b*), during the collapse phase, are shown. As in the case of the O-bearing molecules (Fig. 6), the great chemical differentiation between the two regions is shown by these schematic diagrams. In the Compact Ridge, the relatively high efficiency of the surface saturation processes for oxygen, carbon, nitrogen, and carbon monoxide, leading to the very abundant, and mostly unreactive H_2O, CH_4, NH_3, CH_3OH, and H_2CO molecules, causes the surface reaction pathways related to the production of multicarbon species to be less efficient. From Figure 7*a*, we see that the surface precursor of CH_3CH_2CN, C_3N, is mostly formed in the gas and then accreted onto the grains, where it is successively hydrogenated to form ethyl cyanide. Here, C_3N is not formed via surface chemical pathways as in the Hot Core (see Fig. 7*b*).

The complexity of Figure 7*b*, in which the most important surface processes related to the production of complex N-bearing molecules in the Hot Core are depicted, is primarily due to the higher mobility of carbon and the shortage of hydrogen (both H and H_2) on grain surfaces. The addition of carbon and nitrogen atoms at 40 K, through reactions (3) and (4), becomes a very efficient process that leads rapidly to the formation of the most complex unsaturated species in the model, namely C_9 and C_9N. Once these molecules are formed, saturation starts to be important primarily because hydrogenation remains the only process chemically active. From Figure 7*b* we can see that the final products of the carbon-nitrogen chemistry on the grains, at 40 K, are the most complex organic molecules in the model; these accumulate on the surfaces during the collapse phase because of their low evaporation rates. Note also that surface synthesis of complex species dominates over gas phase synthesis.

To confirm our understanding of how the temperature influences the production of surface multicarbon N-bearing and single-carbon O-bearing molecules, we have run 10 gas-grain pseudo–time-dependent cloud models with fixed density and temperature that differ from each other only in the value of the temperature; the density is fixed at 2×10^4 cm^{-3}. The temperature range considered is 10–100 K, in steps of 10 K. For all these models we chose initial conditions in which hydrogen is molecular in form and considered the abundances of some important surface N-bearing and O-bearing species 10^6 yr after the start of the calculation. In the 10 K model, this time marks the end of the "accretion phase," when the surface abundances begin to dominate the gas phase ones (Hasegawa et al. 1992). The abundances are plotted versus temperature in Figure 8. From Figure 8*a*, we see that abundances of most O-bearing surface species decrease rapidly to chemically insignificant values for $T > 20$–30 K. The complex molecules $HCOOCH_3$ and CH_3OCH_3 show a different behavior, because these surface species are typically formed in the gas

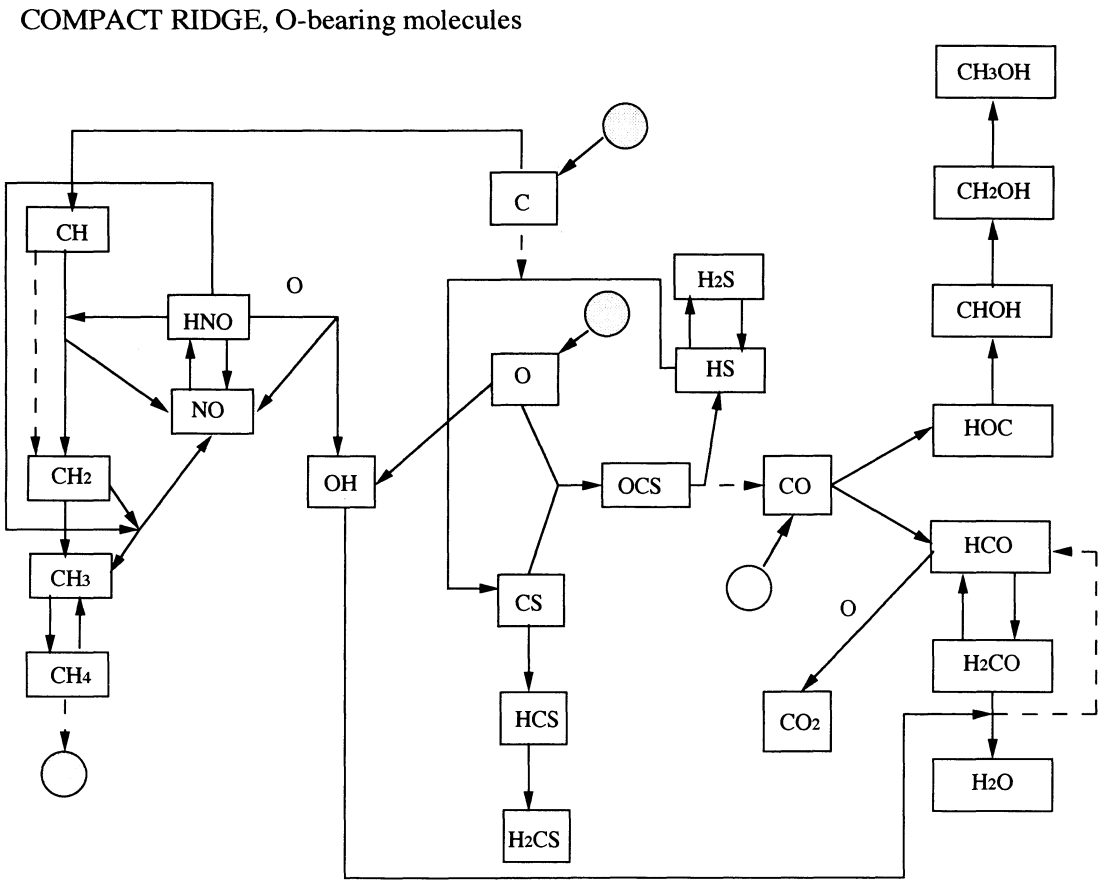

FIG. 6a

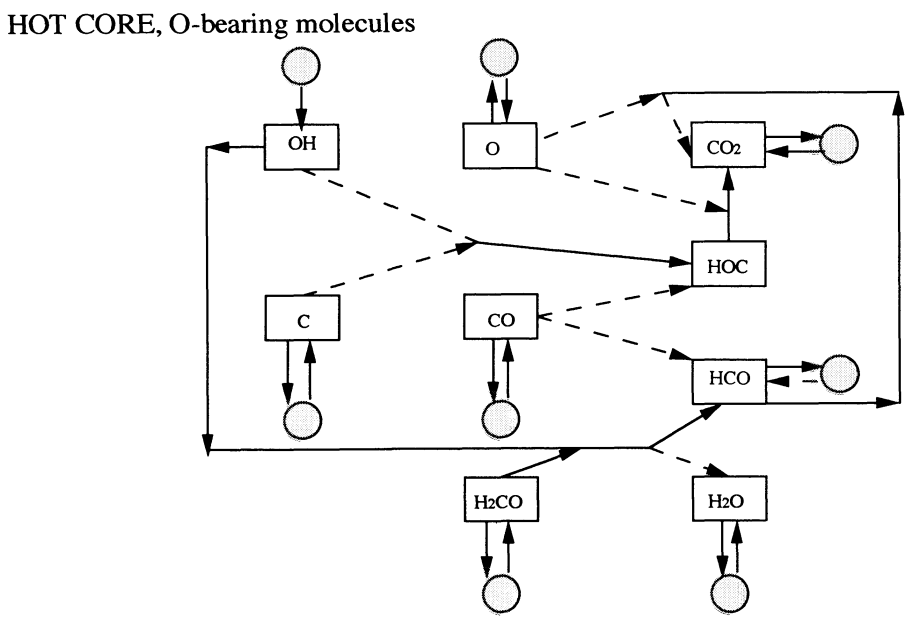

FIG. 6b

FIG. 6.—Formation pathways to O-bearing molecules on grain surfaces during the last stages of the gravitational collapse, before the grain mantle evaporation, for (*a*) the Compact Ridge and (*b*) the Hot Core. The gas species are shown by shaded circles. The dashed lines represent relatively less important pathways. Hydrogen atoms are not shown explicitly.

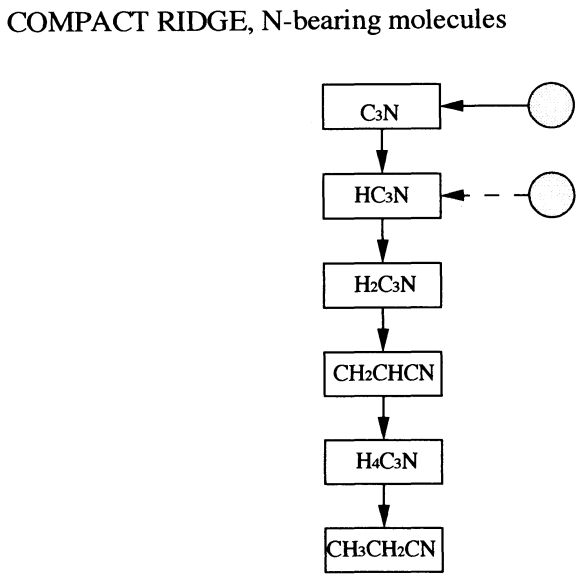

FIG. 7a

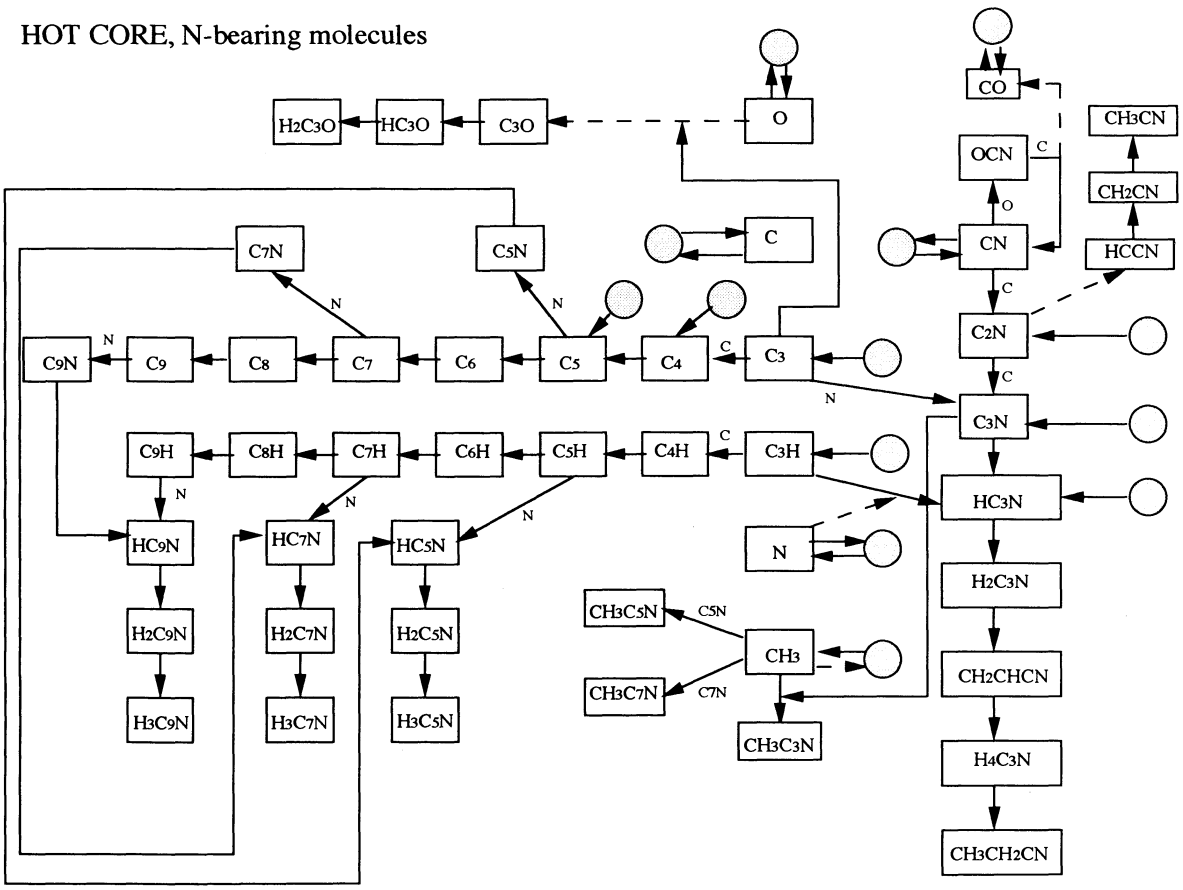

FIG. 7b

FIG. 7.—Formation pathways to N-bearing molecules on grain surfaces during the last stages of the gravitational collapse for (*a*) the Compact Ridge and (*b*) the Hot Core. Otherwise the same as in Fig. 6.

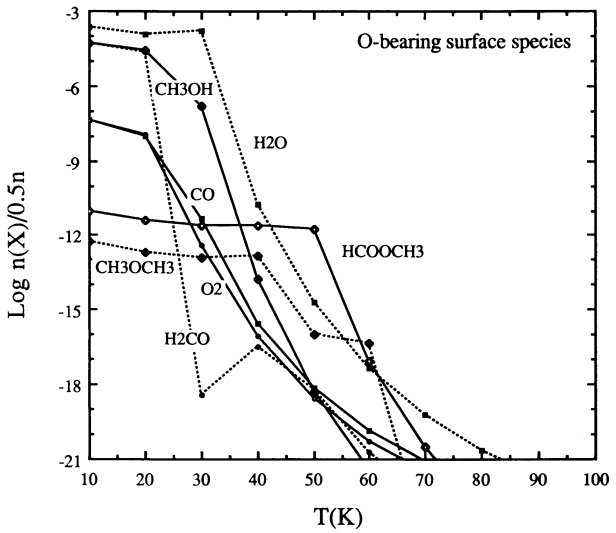

FIG. 8a

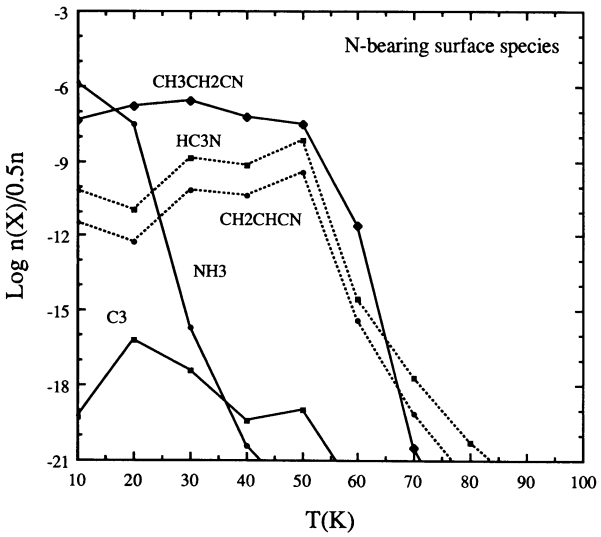

FIG. 8b

FIG. 8.—Temperature dependence of fractional abundances of important (*a*) O-bearing molecules, and (*b*) N-bearing surface molecules at a time of 1×10^6 yr for constant density models.

phase from desorbed methanol (see reactions [10] and [11]). Still, $HCOOCH_3$ and CH_3OCH_3 never achieve large abundances in these low-density models because a high gas phase density of methanol is not achieved. On the other hand, Figure 8*b* shows that the multicarbon N-bearing molecules first increase their abundances as temperature increases, and then decrease rapidly when their evaporation rates, exponentially dependent on temperature, become high enough for complete evaporation of these species from grain mantles; this happens for $T > 50$ K.

5. CONCLUSIONS

In the last few years, several theoretical attempts have been made to understand the observed different spectral signatures in the Orion Hot Core and Compact Ridge, two compact sources close to each other and to the powerful source IRc2. These two regions likely belong to the same molecular cloud from which IRc2 was born, but they show a sharp chemical differentiation: the Hot Core is replete with H-rich N-bearing molecules, whereas the Compact Ridge is mainly characterized by the presence of O-bearing molecules (Blake et al. 1987).

The spatial location of the two clumps (for a good picture of the Orion-KL cloud core see Irvine et al. 1987) suggests consideration of a simple dynamical model in which a massive protostar is accreting material from the cocoon molecular cloud, which possesses a density and temperature gradient (Scoville & Kwan 1976). In our model, the Hot Core and the Compact Ridge are described in an oversimplified manner as two collapsing shells of this cloud at different distances from the central heating source, and therefore at different initial densities and temperatures. At the end of the IRc2 accretion phase, due to radiation, energetic stellar winds, and outflows that interact with the surrounding environment and halt the collapse, the two shells become dense and suddenly hot regions in which the grain mantles evaporate. The results of the chemistry which, following Brown et al. (1988), consists of both gas phase and grain surface processes during the isothermal collapse phase and purely gas phase processes after the regions become hot, are in partial agreement with observations for an isothermal collapse time of $\sim 10^5$ yr and times subsequent to grain mantle evaporation of 3×10^4–1×10^5 yr. The dynamical picture chosen is undoubtedly oversimplified and should be improved.

Several severe discrepancies exist in both sources for some lighter molecules. Perhaps the most serious is the case of ammonia. Although the observed fractional abundance of this species in the Hot Core is large and exceeds its Compact Ridge abundance, our model is unable to produce a large fractional abundance in the Hot Core. Changing the conditions to produce more ammonia on grain surfaces (by starting with atomic hydrogen at a lower temperature) would harm the synthesis of more complex nitrogen-containing species such as C_2H_5CN. The Hot Core abundance of HCN that we calculate is also far too low, because CN is not hydrogenated effectively on grain surfaces.

In the Compact Ridge, the predicted abundance of NH_3 is much too high. This discrepancy can be alleviated if we start with molecular hydrogen rather than atomic hydrogen during the collapse phase. However, if we do so, we approach the chemical development of the Hot Core, in which large amounts of N-containing organics are produced such as C_2H_5CN. Moreover, we initially locate the Compact Ridge at the outer edge of the collapsing cloud where the interstellar radiation field can possibly maintain a high fraction of atomic hydrogen. We also note that, especially for the simpler and more abundant species, there are occasionally uncertainties associated with the observations; given the clumpy nature of the two material condensations, the more extended emission of lighter species can sometimes "mask" contributions from the more compact sources (Blake et al. 1987; Turner 1990). In any case, large H-rich N-bearing or O-bearing molecules do not appear to have an extended counterpart; therefore they stand out in producing the different spectral signatures of the two regions discussed here. Still, it would appear that in attempting to reproduce the distinct organic chemistries of the Hot Core and Compact Ridge sources, we have not been able to account for some of the smaller molecule abundances. Assuming our physical picture of the cloud history to be an accurate one, it would

appear that only a better understanding of grain chemical processes can resolve the dilemma.

Even the distinctiveness of the organic chemistries of the two sources is not totally secure observationally. In particular, the abundance of methanol in the Hot Core may be seriously underestimated by our calculations. Although the multiline millimeter-wave studies of Blake et al. (1987) indicate that methanol intensity peaks in the direction of the Compact Ridge source, and that the methanol rotational temperature and velocity are indicative of this source as well, single-line VLA measurements by Wilson et al. (1989) as well as other millimeter-wave observations by Menten et al. (1988) suggest, on the other hand, comparable abundances of methanol in the two sources. Very recent work by E. C. Sutton using the JCMT in the 345 GHz band (1992, private communication) suggests an order of magnitude greater abundance in the Compact Ridge. A reduction of the temperature in our Hot Core collapse phase from 40 to 30 K can account for the increased methanol abundance, although the overall agreement with observation is not improved. In particular, the abundances of the complex N-containing organic molecules become much too large.

Despite these uncertainties, which may indicate that we have overemphasized the distinctiveness of the two sources, our results do show that thermal effects, particularly efficient in star-forming regions where the dust and gas surrounding a protostellar object are heated above the temperature typical of quiescent clouds, can deeply affect surface abundances, principally through variations in grain surface processes. This can be important in producing the chemical differentiation observed in different star-forming clouds or in different parts of the same circumstellar cloud. A true quantitative understanding of the different chemistries in star-forming regions such as the Hot Core and Compact Ridge sources awaits both more interferometric observations and a better understanding of grain chemistry.

We appreciate the helpful comments of the referee. P. C. acknowledges the support of the Università di Bologna and the partial support of the Ohio State University for a student fellowship. E. H. acknowledges the support of the National Science Foundation for his research program in astrochemistry. We thank the Ohio Supercomputer Center for computer time on their Cray Y-MP/8, and the North Carolina Supercomputing Center for computer time on their Cray Y-MP/4.

REFERENCES

Allen, C. W. 1963, Astrophysical Quantities (London: Athlone), 202
Blake, G. A., Sutton, E. C., Masson, C. R., & Phillips, T. G. 1987, ApJ, 315, 621
Brown, P. D. 1990, MNRAS, 243, 65
Brown, P. D., Charnley, S. B., & Millar, T. J. 1988, MNRAS, 231, 409
Charnley, S. B., Tielens, A. G. G. M., & Millar, T. J. 1992, ApJ, 399, L71
Churchwell, E. 1991, in The Physics of Star Formation and Early Stellar Evolution, ed. C. J. Lada & N. D. Kylafis (Dordrecht: Kluwer), 221
Genzel, R., & Stutzki, J. 1989, ARA&A, 27, 41
Goldsmith, P. F., Irvine, W. M., Hjalmarson, Å., & Elldér, J. 1986, ApJ, 310, 383
Graedel, T. E., Langer, W. D., & Frerking, M. A. 1982, ApJS, 48, 231
Hasegawa, T. I., & Herbst, E. 1993, MNRAS, in press
Hasegawa, T. I., Herbst, E., & Leung, C. M. 1992, ApJS, 82, 167
Henkel, C., Mauersberger, R., Wilson, T. L., Snyder, L. E., Menten, K., & Wouterloot, J. G. A. 1987, A&A, 182, 299
Herbst, E. 1993, in Dust and Chemistry in Astronomy, ed. T. J. Millar & D. A. Williams (NY: Hilger), in press
Herbst, E., & Leung, C. M. 1989, ApJS, 69, 271
———. 1990, A&A, 233, 177
Irvine, W. M., Goldsmith, P. F., & Hjalmarson, Å. 1987, in Interstellar Processes, ed. D. J. Hollenbach & H. A. Thronson (Dordrecht: Reidel), 561
Jacq, T., Walmsley, C. M., Henkel, C., Baudry, A., Mauersberger, R., & Jewell, P. R. 1990, A&A, 228, 447
Johansson, L. E. B., et al. 1984, A&A, 130, 227
Lada, C. J. 1985, ARA&A, 23, 267
Larson, R. B. 1969, MNRAS, 145, 271
———. 1972, MNRAS, 157, 121
Larson, R. B., & Starrfield, S. 1971, A&A, 13, 190
Léger, A., Jura, M., & Omont, A. 1985, A&A, 144, 147
Leung, C. M., Herbst, E., & Huebner, W. F. 1984, ApJS, 56, 231
Magnum, J. G., Wootten, A., Loren, R. B., & Wadiak, E. J. 1990, ApJ, 348, 542
Menten, K. M., Walmsley, C. M., Henkel, C., & Wilson, T. L. 1986, A&A, 157, 318
———. 1988, A&A, 198, 253
Millar, T. J., Herbst, E., & Charnley, S. B. 1991, ApJ, 369, 147
Moore, E. L., Langer, W. D., & Huguenin, G. R. 1986, ApJ, 306, 682
Olofsson, H. 1984, A&A, 134, 36
Pauls, T. A., Wilson, T. L., Bieging, J. H., & Martin, R. N. 1983, A&A, 124, 123
Plambeck, R. L., & Wright, M. C. H. 1987, ApJ, 317, L101
Scoville, N. Z., & Kwan, J. 1976, ApJ, 206, 718
Shu, F. H., Adams, F. C., & Lizano, S. 1987, ARA&A, 25, 23
Spitzer, L. 1978, Physical Processes in the Interstellar Medium (NY: Wiley)
Stahler, S. W., Shu, F. H., & Taam, R. E. 1980, 242, 226
Sweitzer, J. S. 1978, ApJ, 225, 116
Turner, B. E. 1990, ApJ, 362, L29
Walmsley, C. M. 1989, in Interstellar Dust, ed. L. J. Allamandola & A. G. G. M. Tielens (Dordrecht: Kluwer), 263
Walmsley, C. M., Hermsen, W., Henkel, C., Mauersberger, R., & Wilson, T. L. 1987, A&A, 172, 311
Wilson, T. L., Johnston, K. J., Henkel, C., & Menten, K. M. 1989, A&A, 214, 321
Wootten, A., Magnum, J. G., Turner, B. E., Bogey, M., Boulanger, F., Combes, F., Encrenaz, P. J., & Gerin, M. 1991, ApJ, 380, L79
Wright, M., Sandell, G., Wilner, C. J., & Plambeck, R. L. 1992, ApJ, 393, 225